Using AlphaFold and Experimental Structures for the Prediction of the Structure and Binding Affinities of GPCR Complexes via Induced Fit Docking and Free Energy Perturbation

Dilek Coskun[†], Muyun Lihan[†], João P.G.L.M. Rodrigues[†], Márton Vass[‡], Daniel Robinson[‡], Richard A. Friesner[‖], Edward B. Miller[*†]

†Schrödinger, Inc., 1540 Broadway, 24th Floor, New York, New York 10036, United States

‡ Schrödinger Technologies Limited, Davidson House, 1st Floor, Reading RG1 3EU, United Kingdom

‖Department of Chemistry, Columbia University, New York, 3000 Broadway, MC 3110, New York 10036, United States

ABSTRACT: Free energy perturbation (FEP) remains an indispensable method for computationally assaying prospective compounds in advance of synthesis. But before FEP can be deployed prospectively, it must demonstrate retrospective recapitulation of known experimental data where the subtle details of the atomic ligand-receptor model are consequential. An open question is whether AlphaFold models can serve as useful initial models for FEP in the regime where there exists a congeneric series of known chemical matter but where no experimental structures are available either of the target or of close homologues. As AlphaFold structures are provided without a ligand bound, we employ induced-fit docking to refine the AlphaFold models in the presence of one or more congeneric ligands. In this work, we first validate the performance of our latest induced-fit docking technology, IFD-MD on a retrospective set of public experimental GPCR structures with 95% of crossdocks producing a pose with a ligand RMSD ≤ 2.5 Å in the top 2 predictions. We then apply IFD-MD and FEP on AlphaFold models of the somatostatin receptor family of GPCRs. We use AlphaFold models produced prior to the availability of any experimental structure from within this family. We arrive at FEP-validated models for SSTR2, SSTR4, and SSTR5, with RMSE around 1 kcal/mol and explore the challenges of model validation under scenarios of limited ligand-data, ample ligand data, and categorical data.

I Introduction

G-protein coupled receptors (GPCRs) arguably constitute the most important class of drug targets in the human genome. On the order of 35% of known drugs target GPCRs, covering a wide range of crucial disease indications[1]. Furthermore, small molecule candidates targeting previously undrugged GPCRs continue to be introduced into clinical trials, with breakthrough medicines in this category being approved periodically.

Driven by the importance of the GPCR target class, tremendous progress has been made over the past decade in obtaining experimental high-resolution structures of various GPCRs via both x-ray crystallography and (increasingly) cryo-EM spectroscopy. As of December 2022, there are 988 GPCR structures in the PDB, with 916 including a bound ligand[2]. Important insights into the biological functioning of GPCRs have been obtained from these studies, as well as a number of investigations forming the basis for structure-based drug design efforts.

Alongside the experimental efforts outlined above, the revolutionary progress represented by the AlphaFold software platform[3] has engendered the ability to create a plausible structural model even for GPCRs where high resolution experimental structural data is not available. Furthermore, AlphaFold structures have proven to be interesting starting points for computational modeling even in cases of relatively low sequence identity to known experimental structures in the PDB[4].

However, the question of what sort of approach is necessary and sufficient to facilitate structure-based drug discovery efforts for a GPCR requires a different sort of assessment than has been previously carried out. A typical structure-based drug discovery project involves obtaining experimental structures of the receptor complexed with many different ligands, enabling one to track any modifications of the ligand binding mode or receptor conformation during the process of hit-to-lead advancement and lead optimization. Such a protocol can be quite expensive and time consuming (if not infeasible) when the receptor is a GPCR. Furthermore, the plasticity of the GPCR active site poses significant challenges for computational approaches such as protein-ligand docking and free energy perturbation theory[5]. While there has been enormous progress over the past decade in using these methods to discover drug candidates for a wide range of target classes, a successful physics-based computationally driven campaign for a GPCR target has yet to be reported in the literature.

In the present paper, we address the two fundamental challenges associated with carrying out a computationally driven structure-based drug discovery project for a GPCR:

(1) Prediction of ligand binding modes for diverse chemotypes, which requires a robust induced fit docking approach. We carry out these calculations using the recently developed Schrödinger IFD-MD methodology[6], supplemented by the generation of multiple structures with backbone diversity (e.g. from AlphaFold).

(2) Extensive testing of the ability of free energy perturbation (FEP) calculations for ligand series utilizing the induced fit docking structures produced in step (1) to produce correlation with experiment sufficient to be used in lead optimization efforts.

When the binding mode of a novel chemical series to a GPCR is unknown, we argue that FEP calculations can be used to select and validate a specific binding mode produced by IFD-MD. Rigorous validation of this approach will require using the selected IFD-MD/FEP binding mode to prospectively predict the binding of new compounds, the affinities of which can then be measured experimentally.

As an initial test of the IFD-MD methodology when applied to GPCRs, we have developed a data set of 82 pairs of GPCR conformations which exhibit significant induced fit effects, such that accurate cross docking of the ligand from structure A into the receptor conformation of structure B requires, in many cases, the use of an induced fit docking approach. The IFD-MD methodology is successful in 95% of cases in obtaining a structure less than 2.5A RMSD from the native structure for cross docking; the failures generally involve backbone motion which the current algorithm, used in isolation, cannot overcome. We are working on a modified IFD-MD protocol capable of addressing a greater range of backbone motion and will report results for these (and other) test cases in the near future.

To illustrate the application of the IFD-MD/FEP based approach to GPCR targets of current pharmaceutical interest, we have chosen in the present paper to work on the SSTR family of GPCRs. These proteins are currently being investigated as drug targets for a variety of disease indications, and a number of ligand series which bind tightly to the receptor have been published for each of the isoforms[7,8]. Furthermore, the situation with regard to SSTR experimental receptor structures is highly dynamic with new structures being released for SSTR4 and SSTR2 over the past months[9–12]. However, the experimental complex structures that are available are not bound to the ligand chemotypes represented in the various series that we investigate here. Therefore, the situation corresponds precisely to the question posed above: can IFD-MD, in conjunction with FEP be used to identify the binding mode of the series (or multiple binding modes if that is the case), and can FEP achieve a good correlation with the experimental binding data for the series across a wide range of congeneric ligands?

We investigate the ability of both experimental structures (crystal structures and cryo-EM structures) and AlphaFold structures to enable successful IFD-MD docking and FEP simulation. Exploration of multiple starting structures for a given ligand series enables ligand binding poses to be found which enable very good correlations to be obtained between FEP calculations and the experimental binding (or functional assay) data. As noted above, rigorous validation of the proposed binding mode would require prospective FEP prediction using the model, and experimental assessment of the ligands selected for synthesis from these calculations. If more than one competitive model is identified, synthesis and testing of ligands which have substantially different binding affinity predictions in the alternative models can resolve which model is correct. Our results suggest that the correct binding mode can be identified via the proposed combination of computational and experimental work, but unambiguous establishment of the viability of this approach awaits application in the context of an ongoing project.

A key finding of the present study is that relatively small helix motions of the receptor can play a critical role in enabling the ligand to dock in a particular binding mode. Docking into multiple structures can yield a successful induced fit binding pose prediction as long as at least one of the structures has the required helix conformations. An alternative to relying on AlphaFold and/or experimental structures is to computationally enumerate low-energy helix configurations, for example using steered molecular dynamics and/or various conformational search algorithms A more systematic approach to sampling a wide range of relevant GPCR helix configurations, minimizing the dependence upon a small number of input structures, is the subject of current investigations in our group. For the present, a combination of utilizing an ensemble of AlphaFold structures, in conjunction with simple helix perturbations, should enable IFD-MD to handle some (if not most) cases of practical interest in structure based GPCR drug discovery projects.

The paper is organized as follows. In Section II, we present IFD-MD retrospective testing using pairs of complexes, across a wide range of GPCRs, from the PDB. Section III develops binding pose models for three different SSTR receptors (SSTR2, SSTR4, and SSTR5) for a number of ligand series, and demonstrates that FEP calculations using these models correlate well with experimental data. In Section IV, we consider the limitations and their remedies of this approach in active drug discovery projects. Finally in Section V, we summarize our results and outline future directions.

II Retrospective IFD-MD Performance for GPCR structures in the PDB

We first obtain a list of all public ligand-bound GPCR structures from the GPCRdb[2], and download both the 3D coordinates and the structure validation report for each from the RCSB PDB. Then, using a high-resolution structure of the A2A receptor (PDB ID: 6wqa) as a reference, we filter out structures lacking ligands occupying the orthosteric binding pocket. In addition, we also discard structures with global resolution worse than 3.5 Å or with poorly resolved, incomplete, or multi-conformer binding pocket residues (binding pocket residues are defined as those having at least one heavy atom within 5 Å of the ligand). To prepare for cross-docking, the processed structures are then grouped by Uniprot ID of the receptor and discarded if they do not have at least one additional structure with the same Uniprot ID. For each set of Uniprot-grouped receptors, we analyze all pairwise combinations of structures, grafting the ligand of the target structure onto the pocket of the template receptor, after aligning the receptors using CEAlign[13]. These pairs are filtered for cases where the template and target receptors are either too similar (sidechain RMSD below 1.0Å) or too different (backbone RMSD above 1.5Å), where there were either no sidechain clashes between the template receptor and the target ligand (no induced fit necessary), or where there were large clashes between the template receptor backbone and the target ligand. The resulting subset of structures are processed using the Schrodinger PrepWizard tool[14], in order to add hydrogen atoms, define protonation states for titratable groups, and perform a restrained minimization. This analysis yields a total of 82 pairs across 10 different GPCRs that cover a wide spectrum of subtle binding pocket rearrangements. No parameter optimization is performed for either IFD-MD or GlideSP in obtaining these results; the parameters remain robust across target class. Methodologically, an explicit membrane treatment was added to IFD-MD which we discuss now.

Table S1 lists the individual cross docks and the performance of GlideSP (rigid receptor docking) and IFD-MD. Overall performance is shown in Figure 1. As we note above, these cases are deliberately selected because of an observed induced-fit effect primarily due to side chain motion. The rigid-receptor docking results serve as a benchmark of the difficulty of these cases as, in some instances, the ligand is able to contort itself around the rigid receptor conformational perturbation and preserve a ligand RMSD better than 2.5 Å. As in our prior work[6,15], we define success to be a ligand RMSD of 2.5 Å or better found within the top 2 ranked predictions. With only 49% of cases succeeding using GlideSP, we conclude that more than half the remaining cases are not solvable with rigid-receptor docking.

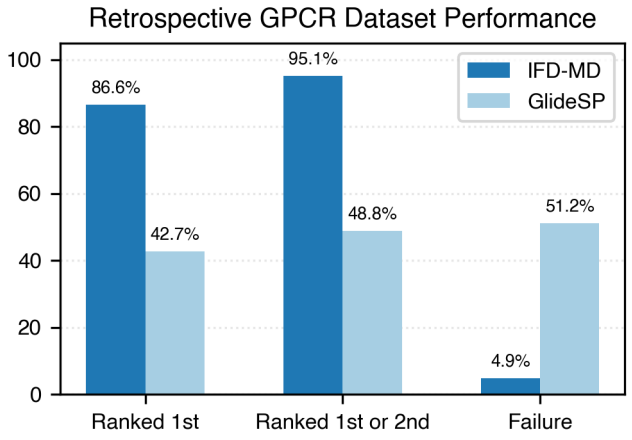

Figure 1. Retrospective GPCR performance across a set of 82 cross docks spanning 10 targets. Success is defined to be a ligand RMSD of 2.5 Å or better in the top two predictions.

Briefly, we summarize the IFD-MD protocol as consisting of two halves. First, an implicit solvent half which utilizes iterative rounds of pharmacophore docking, rigid-receptor docking, and binding site optimization (side chain reprediction and backbone minimization). The second half of IFD-MD incorporates short 500 ps MD to relax the entire system around the predicted pose followed by scoring with a modified form of a water-aware rigid-receptor docking scoring function, WScore[16], and 10 ns metadynamics trials[17] to test the relative stability of competing binding modes. If we find that the 500 ps simulation deviates significantly from the pose prior to MD, we consider the system unconverged and run an additional 100 ns of MD. For membrane proteins, we modify the original IFD-MD protocol[6] to include an explicit representation of the membrane during the unbiased molecular dynamics and metadynamics simulation stages. Specifically, we use a reference structure, e.g. downloaded from the OPM database[18], to define the orientation and thickness of the membrane. This structure can be of the same receptor, unliganded or bound to a different ligand, or of a homologue. When preparing the predicted models for simulation, the backbone atoms of the receptor are aligned to this reference structure using CEAlign[13]. The implicit solvent model approximates the solvation free energy using a variation of the surface generalized Born model with a variable dielectric, VSGB2.0[19]. When adding an explicit membrane, we use this pre-aligned structure and the membrane thickness information to build a POPC bilayer during Desmond (molecular dynamics) system setup[20,21]. Finally, the full system consisting of the receptor, ligand, membrane, solvent, and neutralizing ions is equilibrated using a version of the Schrödinger membrane relaxation protocol[5,22] modified to include GCMC[23] stages to solvate the binding pocket.

These retrospective results demonstrate the performance of IFD-MD on a range of GPCR target classes and specific receptors. When starting from an experimentally obtained structure, as we show above, the IFD-MD scoring function achieves success within the top two predictions. But starting from a template-based homology model or an AlphaFold model, the geometry of the binding site can contain errors that erode the utility of the IFD-MD scoring function. As we showed in a prior publication[15], when evaluating template-based homology models across various sequence identities, a robust approach is to explore the top five predictions with FEP validation. In the sections that follow we build off this prior work by challenging AlphaFold models of GPCRs for which there are no close experimental homologues and validate the models by recapitulation of experimental activity data using FEP, exploring the top 5 IFD-MD poses for each AlphaFold model as outlined above.

III Evaluation of AlphaFold models of the Somatostatin receptor family of GPCRs

The somatostatin receptor family, a class A GPCR family, is composed of five members numbered SSTR1 – SSTR5[24]. At the time that we queried AlphaFold for structures from this family, January 27th 2022, there were no experimental structures of any member of this family. The nearest experimentally solved homologues are the μ and ∂ opioid receptors at around 40% sequence identity. Therefore, the somatostatin family offered an opportunity to challenge AlphaFold models for a target for which no possibility exists for AlphaFold to have been trained on any experimental solution, nor of any close homologues. There have since been experimental structures reported for SSTR2 and SSTR4, and below we compare our final models with these experimental structures, however these structures do not contain bound any chemical matter congeneric to the datasets discussed here.

III.A Dataset construction

Model evaluation requires a ligand dataset, however the characteristics of the available data for any given target will be quite variable. To account for this type of variability our data comes from three different publications and consists of a high-quality large dataset (SSTR4), a smaller but still high-quality dataset (SSTR2) and a large, but lower-quality dataset (SSTR5). For SSTR4, we select a 2016 patent application concerning agonists targeting SSTR4[25]. The publication consists of 79 small-molecule ligands with EC50 data spanning an activity range of 0.6 nM to 2 μM. Figure 2A shows the Markush structure of this series. Of the 79 ligands, we pick the largest subseries that contains 64 compounds with the Y-W groups representing either 5-6 or 6-6 fused rings. We exclude ligands with unknown stereochemistry.

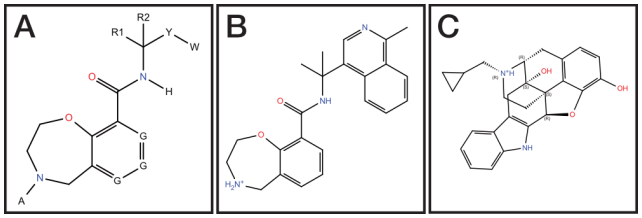

Figure 2. Template ligand and target ligand for SSTR4 modeling. A) Markush structure from Mazzaferro et. al., the patent publication containing the SSTR4 ligand dataset. B) The most potent ligand from the SSTR4 6-6 subseries. This ligand is the initial target ligand for IFD-MD. C) Naltrindole, the template ligand taken from PDB ID 4N6H, a ∂-opioid structure.

This dataset is well suited for model evaluation because of its large size (> 30 ligands) and large activity range (around 4 kcal/mol). Datasets with these characteristics do not perform well under the use of null models, such as random assignment of predicted ΔG around the mean[15,26], offering a stark contrast compared to a successfully predictive model.

For SSTR2, we explore the ability of our methodology to achieve model validation with a far more limited data set. Here, we select a publication describing small molecule agonists[27]. The paper contains 18 ligands with K_i data spanning 1.8 nM to 2.8 μM. While the activity range is excellent, the limited number of ligands results in two competing predicted models which, without additional compounds, could not be distinguished further. This is discussed further below.

Finally, for SSTR5, we explore the use of categorical, rather than quantitative, data. Here, we select a 2019 patent application describing a large set of 346 congeneric ligands which are agonists to SSTR5. While the quantity of data is large, the quality is limited as the degree of agonism is expressed by assigning each ligand to one of four categories: a) EC_{50} < 10 nM, b) EC_{50} from 10 to 100 nM, c) EC_{50} from 100 to 1000 nM, and d) EC_{50} > 1000 nM. Furthermore, the ligands are not evenly distributed among the four categories; 80% of the ligands are in the open-ended category *a*. Validation of models with this dataset requires careful selection of model discriminating edges, for example, the smallest perturbation between pairs of ligands which span categories. We elaborate on this further below.

III.B Modeling SSTR4

The most robust dataset (combining quantity of ligands and quality of experimental binding affinity measurements) is that for SSTR4. The overall procedure is to dock one or more ligands from the congeneric series into one or more AlphaFold models of that target and to then perform retrospective free energy perturbation calculations. Based on numerous past publications starting from both high resolution crystal structures and retrospective template-based homology models with between 30-50% sequence identity, the correct induced fit model of the ligand series should, with a sufficiently large ligand series, demonstrate a clear signal with low RMSE and high R^2, and an incorrect model should lack these qualities[4,15,28–31].

We begin by noting that no single AlphaFold model, nor for that matter a single model of any provenance, will be suitable for binding all known potent chemical matter for that target; induced fit effects are always a possibility. Our previously published algorithm, IFD-MD, has been shown to achieve over 90% accuracy in producing a 2.5 Å ligand RMSD pose within the top two ranked predictions[6]. The induced-fit effects in this prior publication all required at least one alteration of the receptor side chain rotamer states. In the most challenging cases, the necessary induced-fit motion also includes some backbone motion; the current IFD-MD algorithm can often handle this as long as the motions required are not too large. Between the dynamical and non-dynamical sampling within IFD-MD and with the enhanced sampling performed during the FEP calculations, there exists some wide but quantitatively unknown radius of convergence between the starting IFD-MD model and the final, FEP performant model.

In the present work, we seek to further broaden our radius of convergence with regard to backbone variation by initiating docking, not from a single model, but from the top five structural models produced by AlphaFold. For each of these five initial AlphaFold models, we perform an IFD-MD calculation, selecting the 5 best scoring IFD-MD models with the ligand bound into the orthosteric GPCR binding site. This leads to a total of 25 models for which we perform FEP testing.

IFD-MD requires a template-ligand as part of its input. This is a ligand, placed in the initial receptor model, that serves two purposes – it defines the binding site, and it provides a pharmacophore model which is used to aid the earliest part of the docking. In a typical cross-docking experiment, the template ligand is some other ligand bound to the same target; here we lack any experimental structure of SSTR4. Following the same approach that we took for evaluating template-based homology models[15], we graft the ligand from the closest experimentally solved homologue into the model binding site. For SSTR4, we graft the ligand from PDB ID 4N6H, Naltrindole, bound to the ∂ opioid receptor, into the AlphaFold SSTR4 models after performing a structure alignment. This ligand is shown in Figure 2C.

Schrödinger's free-energy perturbation package, FEP+, is then used to predict the protein-ligand binding affinities across a ligand congeneric series[26,32]. Default FEP settings are used with the exception that 25 ns of simulation time are performed instead of 5 ns. The default protocol consists of 12 lambda windows and 24 lambda windows for charge perturbations. Replica exchanges between neighboring windows are attempted every 1.2 ps. The default map generation protocol is used which is a variant of the LOMAP mapping algorithm[33]. Each edge is nested within at least one closed cycle and there is at least one path containing fewer than five edges between any pair of compounds.

A significant body of evidence, predating the availability of any SSTR structure, has indicated that LYS-9 in somatostatin is crucial for activity[34] (recently structures of somatostatin bound to SSTR2 have confirmed this[35]). Furthermore, in the SSTR ligand datasets that are used here, a primary or secondary amine is always kept constant within each series[27,36,37]. We operate under the assumption that mimicking LYS-9 in somatostatin, the biologically active state within the ligand dataset here has the primary or secondary amine positively charged. We therefore perform our simulations with the ligands positively charged and assume the neutral bound form does not significantly contribute to the pKa-corrected ΔG. This allows us to avoid a 2X increase in compute cost by avoiding FEP simulation of the neutral form of each ligand.

Given the requirement that the secondary amine within the oxazepine (the 7 membered aliphatic ring) must be protonated in order to bind to the receptor, the pKa of this group across the congeneric series becomes a quantity that can significantly impact the binding affinity. Calculated pKa values, computed using Schrödinger's Jaguar Macro-pKa[38] Workflow in the 2023-2 release[39], indicate significant variation in the pKa as a function of the position of a nitrogen atom in the fused phenyl ring (the G positions in Figure 2A). As the pKa varies, a ΔG correction is necessary to account for the free-energy cost of protonating the ligand when the oxazepine nitrogen is preferentially in the neutral state[40] when isolated in solution. Table S2 lists the predicted pKa for the tertiary amine, and the corresponding free energy correction added to the FEP results, as a function of the position of a nitrogen in the fused phenyl ring.

As we are evaluating five AlphaFold models of SSTR4 and each IFD-MD job can produce up to 5 predicted ligand-receptor complexes, we have a total of 25 models to evaluate in FEP. It is unnecessary to perform FEP on the entire congeneric series immediately – a hierarchical approach is more practical because the performance of a subset of ligands should be enough to quickly discard several models. It is an active area of further research to find out what the smallest subset would be for efficient model discrimination. In this work, we first evaluate the performance of the models using the complete but smaller single subset of 18 ligands referred to as the 6-6 sub-series. This sub-series is defined by the Y-W positions shown in Figure 2a being a fused 6-6 ring. We select as the target ligand, which is the one ligand which is explicitly docked using IFD-MD, to be the most potent ligand from this sub-series. This is ligand **27** from the patent[25], shown in Figure 2B and has a reported EC_{50} of 0.6 nM. As can be seen, this ligand is not congeneric to the template ligand from the ∂ opioid receptor Figure 2C.

Table 1 shows the performance for these 25 IFD-MD models in FEP and includes the pKa corrections described above. Out of the 25 models, only three models lead to an RMSE of near 1 kcal/mol. These models are (AF5, IFD1), (AF4, IFD2) (AF5, IFD4). The nomenclature where use here is that (AF5, IFD1) refers to the top-ranked IFD-MD model obtained from docking into the 5th ranked AlphaFold model. We must now test the performance of these models by including the remaining 46 ligands from the 5-6 fused ring sub-series.

Table 1. FEP performance of the IFD-MD outputs run on AlphaFold models of SSTR4 using the 18 ligands from the 6-6 fused ring sub-series[a]

	FEP Performance R^2 / $RMSE_{pairwise}$ (kcal/mol)				
IFD-MD Rank	**AF Rank**				
	1	**2**	**3**	**4**	**5**
1	0.01 / 1.79	0.26 / 1.31	0.07 / 1.93	0.01 / 1.90	**0.57 / 0.97**
2	0.32 / 1.64	0.02 / 2.16	0.21 / 1.70	**0.24 / 1.19**	0.03 / 2.29
3	0.24 / 1.96	0.06 / 1.85	0.17 / 1.68	0.01 / 1.55	0.00 / 2.14
4	0.24 / 1.47	0.22 / 1.42	0.11 / 1.93	0.00 / 1.86	**0.55 / 0.91**
5	0.02 / 1.66	0.34 / 1.29	0.32 / 1.40	0.18 / 1.24	0.01 / 1.78

a. R^2 is the coefficient of determination between experimental ΔG and predicted ΔG. $RMSE_{pairwise}$ is the root-mean-square error compared to experiment of the FEP values with respect to the relative free energy change for all ligand pairs.

We align the 46 ligands from the 5-6 subseries onto these top three models. Table 2 lists the performance of the models with 46 of these ligands included for a total of 64 ligands.

Table 2. FEP Performance for the complete 5-6 and 6-6 subseries on the top models determined from 6-6 subseries.

Model	**FEP Performance**	
	R^2	**$RMSE_{pairwise}$ (kcal/mol)**
AF5, IFD1	0.54	1.00
AF4, IFD2	0.44	1.14
AF5, IFD4	0.57	0.96

With the complete set, only two models appear competitive (AF5, IFD1 and AF5, IFD4). For additional validation, we perform absolute-binding FEP (AB-FEP) calculations for each model. AB-FEP is independent of the size of the congeneric series and can serve as a complementary calculation for model validation[15,41].

Table 3. Comparison of AB-FEP predicted ΔG versus experiment for most potent 5-6 ligand, example 33

Model	**AB-FEP Predicted ΔG (kcal/mol)**
AF5, IFD1	-13.24
AF5, IFD4	-6.05
Experimental ΔG	-12.48

Table 3 lists the results of the AB-FEP calculation on the most potent 5-6 ligand. An overprediction of the binding free energy is preferred as AB-FEP does not take into account the non-negative reorganization free energy from the receptor's apo to holo state[41]. Therefore, the result for the AF5, IFD1 model is reasonable while the AF5, IFD4 model appears unlikely to be correct as it is underpredicting the experimental binding affinity by more than 6 kcal/mol. We conclude that AF5, IFD1 is our best and final model.

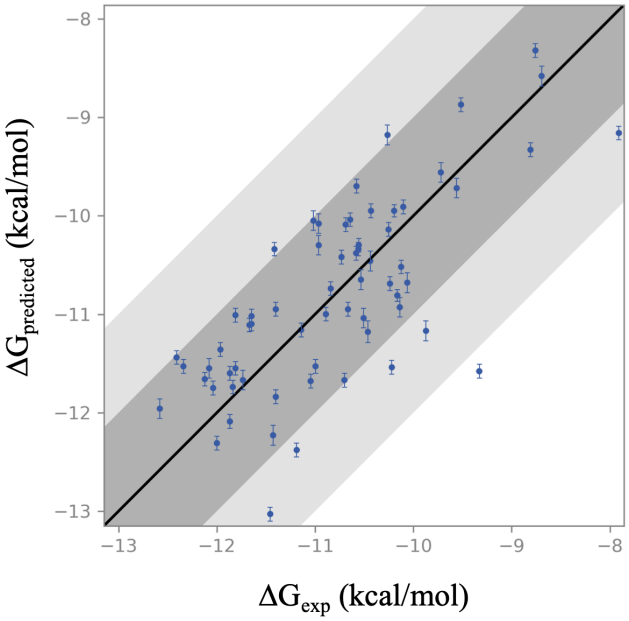

Figure 3. Plot of predicted ΔG versus experimental ΔG for the final SSTR4 model. This model contains all 64 ligands combining both the 5-6 fused ring sub-series and the 6-6 fused-ring subseries. The R^2 is 0.54 and the $RMSE_{pairwise}$ is 1.00 (kcal/mol).

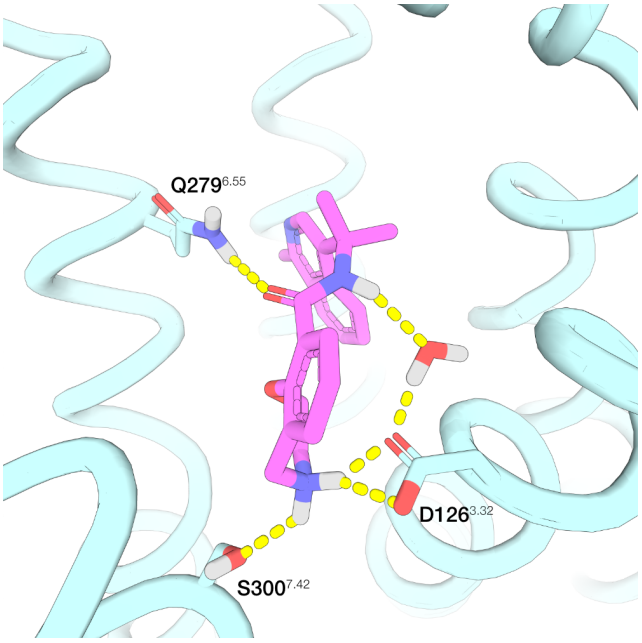

Figure 4. Final predicted binding mode for the most potent ligand in the patent application, ligand ***27***. Shown in dotted lines are the hydrogen bonds involving the ligand. The ligand forms a salt bridge to D126. Hydrogen bonds are formed to S300 and Q279. A second water-mediated hydrogen bond is formed to D126.

Our final model predicts a salt-bridge between the conserved positive amine in the ligand and ASP126. The ligand amide NH also forms a water mediated interaction to ASP126. Additional hydrogen bonds are formed to S300 and Q279. These interactions are shown in Figure 4 and the plot correlating experimental ΔG with FEP predicted ΔG is shown in Figure 3.

III.C Analysis of the predicted SSTR4 holo-protein

With the completion of a single model that satisfactorily recapitulates experimental activity data for 64 ligands, we now turn to a physical analysis of this model. First, we seek to address what induced fit motion was necessary for this binding mode compared to the original AlphaFold models. Secondly, since the completion of this predicted model, an experimental structure of SSTR4 bound to a small molecule agonist has been published, PDB ID 7XMT. The small molecule in this structure is unrelated to the one in the patent dataset that we use and so it remains the case that no public experimental structure exists of SSTR4 bound to the agonist series discussed in this work.

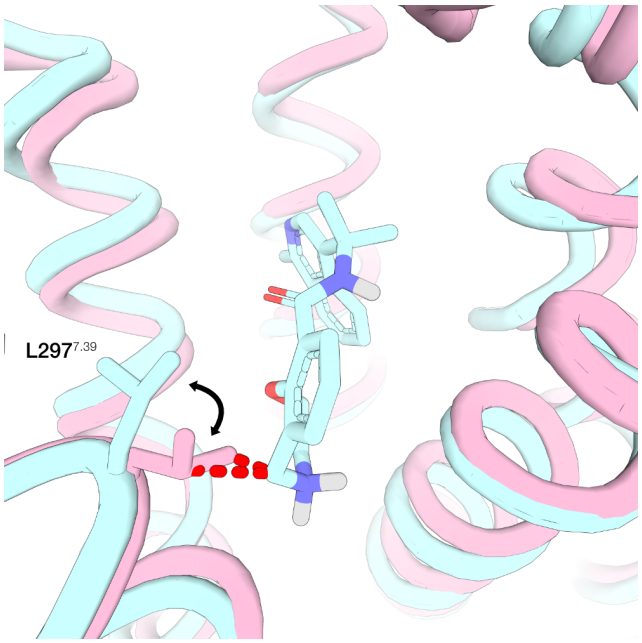

Figure 5. Comparison of the final predicted SSTR4 liganded structure (cyan) and the original AlphaFold model 4 (pink). The most significant induced fit effect is the motion of LEU297.

Figure 5 shows a comparison between the final predicted SSTR4 liganded structure and the original AlphaFold model from which it originated: the 5th ranked AlphaFold model (AF5). For this model, the original position of L297 clashes with the predicted position of the ligand's secondary amine. The motion of L297 is the predicted induced fit effect necessary to achieve the final model. Attempts to use rigid-receptor docking (GlideSP[42]) into the 5th ranked AlphaFold model show that no model is obtained which can form the salt bridge with Asp126 when Leu297 is unmoved (Figure S1).

While we understand precisely the induced fit motion necessary if starting from AF5, it is less clear precisely what motion is necessary for the other AlphaFold models 1-4. In Table 2 we listed the FEP performance for the full 64 ligands on the top three IFD-MD models. The least competitive model of the three, (AF4, IFD2) is actually quite similar to our best model with a 1.2 Å RMSD and yet the FEP performance is inferior with R^2 degrading from 0.54 to 0.30. Figure 6 shows these models in the binding site. This model starts from the 4th ranked AlphaFold model which contains a small helix 7 tilt that drags

TYR301 slightly into the binding pocket. The ligand makes a compensatory translation but in doing so is unable to form the hydrogen bond to SER300. We hypothesize that details of this magnitude affect the FEP performance and that other similar helix motions, beyond the scope of IFD-MD's sampling, render AlphaFold models 1-4 presently unsalvageable.

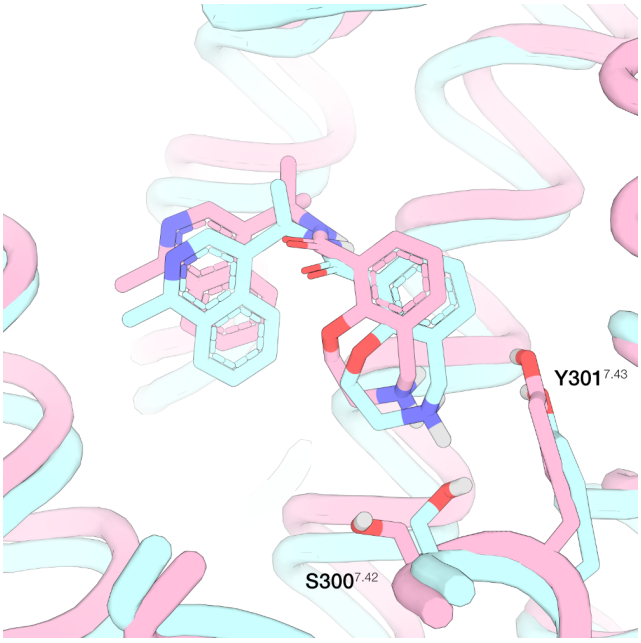

Figure 6. Comparison of two of the top IFD-MD AlphaFold models. In cyan is our top model (AF5, IFD1), in pink is our third best model (AF4, IFD2). A small helix tilt around TYR301 forces the ligand to translate slightly further out of the pocket. This removes the ability for the ligand NH2 to form a hydrogen bond to SER300.

Finally, we discuss the use of PDB ID 7XMT as an input structure for IFD-MD. This SSTR4 experimental contains the non-peptidic agonist J-2156[12] which is non-congeneric to any of the ligands in the patent dataset used here. This structure was published after we used AlphaFold to produce our models and offers an opportunity to compare performance starting with an experimental SSTR4 structure bound to a small molecule. Using this structure as an input to IFD-MD we produce five structures and perform FEP using the smaller 18 ligand 6-6 fused ring subseries.

Table 4. FEP Performance for the 6-6 fused ring sub-series using IFD-MD starting from PDB ID 7XMT

IFD-MD Model from 7XMT	FEP Performance for 6-6 sub-series R^2 / $RMSE_{pairwise}$ (kcal/mol)
IFD1	0.58 / 0.89
IFD2	0.00 / 1.93
IFD3	0.04 / 2.28
IFD4	0.01 / 2.02
IFD5	0.06 / 2.32

Table 4 shows the FEP performance on the 18-ligand 6-6 fused ring subseries on all five IFD-MD outputs starting from 7XMT. The top-ranked pose, IFD1, is the only one showing any signal, with an RMSE of 0.89. The binding mode of this model is very similar to our final AlphaFold/IFD-MD model with a ligand RMSD of 1.12 Å and is shown in Figure 7. We take this recapitulation of our best AlphaFold model in this experimentally derived structure as supportive of our proposed model being correct.

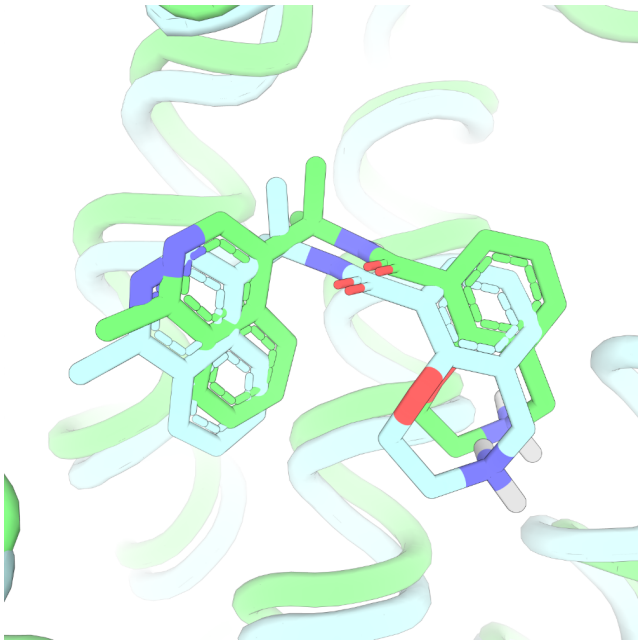

Figure 7. Comparison of the predicted binding mode of our final AlphaFold-IFD-MD structure (cyan) and 7XMT-IFD-MD structure (green). The two binding modes have a ligand RMSD of 1.12 Å between them.

III.D Modeling SSTR2

Modeling SSTR2 presents the challenge of FEP validated structure prediction with a limited congeneric series data set. The dataset here comes from *Contour-Galcéra* et. al 2005, describing 18 congeneric ligands with K_i reported ranging from 1.8 nM to 2.8 μM[27].

As in our modeling for SSTR4, we generated five AlphaFold SSTR2 models on March 3rd, 2022, preceding the release of any public SSTR structures. We graft the ligand from PDB ID 5C1M, a μ-opioid receptor structure, into each of the AlphaFold models and dock the most potent ligand, labelled ***5o*** in the reporting publication, into each of the five AlphaFold models. Table S3 reports the FEP performance of the IFD-MD models produced using the five AlphaFold models. We quickly arrive at a single model with superior performance, AlphaFold Rank 2, IFD-MD Rank 4. This model produces an R^2 of 0.78 and an RMSE of 0.95 kcal/mol.

Since the generation of this model, multiple SSTR2 experimental structures have been deposited in the PDB. We select four of them to use as input to IFD-MD followed by FEP. None of the experimental structures used here, nor since released in the PDB contain a small molecule congeneric to the dataset used herein. Table S4 shows the performance across these four

experimental structures. A single model stands out with superior performance. This model is the 5th ranked output of IFD-MD starting from PDB ID 7T11. The R^2 is 0.70 and the RMSE is 1.31 kcal/mol.

Figure S2 shows the FEP correlation plots for our best AlphaFold derived model and the derived model from 7T11. This model derived from 7T11 is slightly inferior in terms of relative FEP statistics but given the small size of the dataset (18 ligands) we proceed anyway with AB-FEP calculations using ligand **5o**. The AB-FEP calculations produce a contradictory result with the AlphaFold derived model yielding an AB-FEP ΔG of -19.8 kcal/mol versus -21.94 kcal/mol using the structure derived from 7T11. For comparison the experimental ΔG is -11.93 kcal/mol indicating that both AB-FEP predicted ΔG's are plausible accounting for the non-negative, but unknown, protein reorganization free energy cost to obtain the holo receptor conformation. The AB-FEP ΔΔG between the two models is 2.14 kcal/mol, however, ligands forming strong salt-bridge interactions with the receptor are known to have challenging convergence for absolute binding FEP[41] of which our SSTR2 binding modes certainly fall under. We would prefer to see relative and absolute binding FEP agree before declaring a final model.

Surprisingly, this model derived from 7T11 and the model derived from AlphaFold are significantly different. Figure 8 shows this comparison. Among other differences, the 7T11 model has a hydrogen bond between the core triazole and T194 in the ECL2 loop. The AlphaFold derived model lacks this interaction.

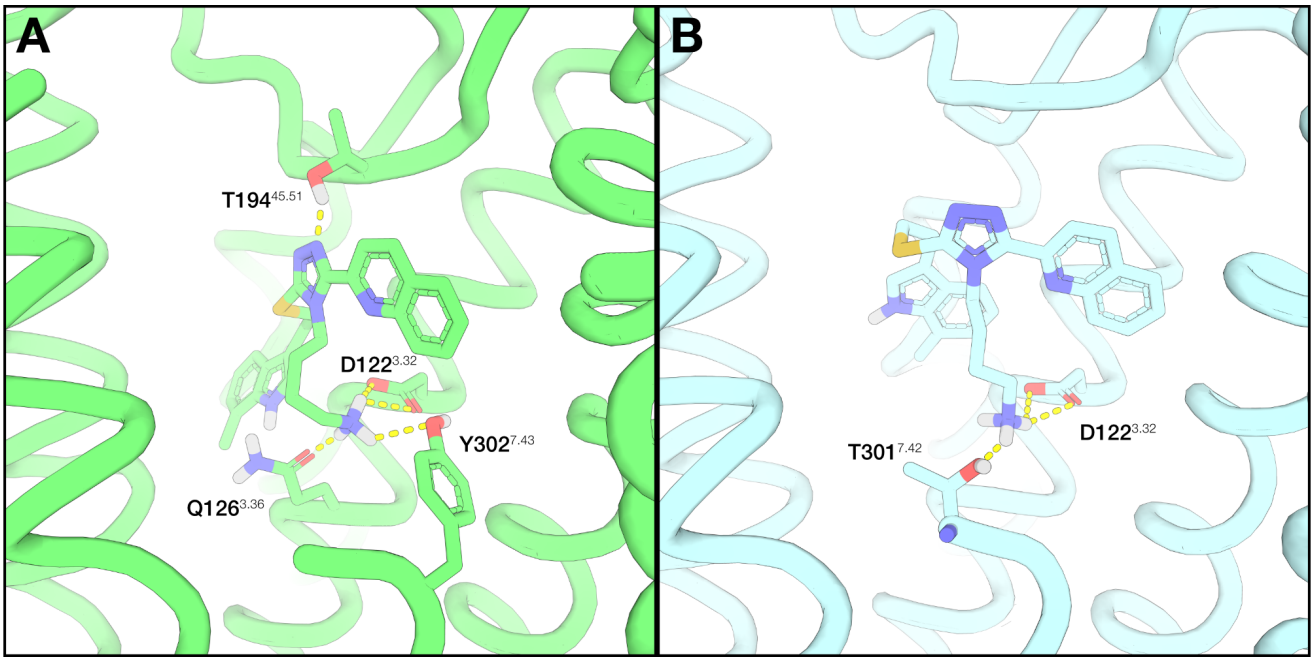

Figure 8. Comparison of the final models of SSTR2 bound to ligand *5o* in *Contour-Galcéra* et. al 2005. A) The final model generated starting from PDB 7T11, a cryo-EM structure of SSTR2 B) The final model generated starting an AlphaFold Model.

Without the benefit of additional assayed congeneric ligands, or perhaps the need for additional modeling, we cannot conclusively select which model is correct. We note however that in an active project this is not a fatal limitation; additional compounds can be rationally designed to challenge both models and potentially arrive at a final, single model.

III.E Modeling SSTR5

For SSTR5, we cope with the challenge of FEP validation structure prediction using a categorical dataset. Such a dataset does not provide absolute affinity or functional activity measurements, for example, a K_i of 100 nM, rather each ligand within a given congeneric series is reported as belonging to a category and that category is defined as encompassing a range of EC_{50} values. For the patent[37] that we use here, there are four categories for EC_{50} activity: a: <10 nM, b: 10-100 nM, c: 100-1000 nM, d: >1000 nM.

Crucially, there is no single ligand with a quantitative EC_{50} to serve as a reference in relative FEP to convert the predicted ΔΔG values into a ΔG. Therefore, other than arbitrarily assigning a reference EC_{50} that lies within a single category, we are restricted to using only ΔΔG values to evaluate our models' performance. To use ΔΔG values, FEP calculations between two ligands in an open-ended category are useless. For example, in category *d*, an open-ended category for ligands with an EC_{50} > 1000 nM, if one uses FEP to predict the ΔΔG of two ligands in this category, any predicted ΔΔG value would appear satisfactory. In one model, a ΔΔG of +1.37 kcal/mol between two category *d* ligands could be interpreted that one ligand is 2 μM, and another ligand is 20 μM. Note that 1.37 kcal/mol is the free energy needed to achieve a log-order change in binding affinity at 300K. Yet, in another model, that same pair of ligands could be predicted to have a ΔΔG of +2.74 kcal/mol, implying one ligand is 2 μM and another ligand is 200 μM. Both models satisfy the definition of category *d* and therefore a predicted ΔΔG between these pairs of ligands cannot be used to discriminate between competing models.

The only pairs of ligands which can productively be used for model discrimination are those which differ by more than one category. Comparing a ligand in category *a* (< 10 nM) with a ligand in category *c* (100 – 1000 nM), the smallest correctly predicted ΔΔG, a lower bound, must be +1.37 kcal/mol in perturbing from the *a* ligand to the *c* ligand. This could correspond to the ligand in category *a* having an EC_{50} of 10 nM and the ligand in category *c* an EC_{50} of 100 nM. A ΔΔG more negative than +1.37 kcal/mol would be incorrect and any ΔΔG more positive than +1.37 would satisfy the categorical definitions. Specifically, a predicted ΔΔG of + 2 kcal/mol could be considered to have an error of 0 kcal/mol, while a predicted ΔΔG of +1 kcal/mol could be in error by at least 0.36 kcal/mol. We call this type of calculation the "lower-bound" error and summarize the performance of all predicted ΔΔG's for a model with a lower-bound RMSE ($RMSE_{lower\text{-}bound}$). This becomes the metric by which we evaluate models using this categorical dataset.

The dataset for this patent application, in addition to being categorical, is not optimally balanced among the categories. After removing ligands with multiple possible chiral states, tautomers and protonation states we are left with 164 ligands out of the total of 364 reported in the patent application. Of these 164, the breakdown by category is: *a*) 139, *b*) 11, *c*) 7, *d*) 7. Thus over 84% of the ligands are in the open-ended most potent category *a*. Not every ligand pair spanning non-adjacent categories is trivial to run; large, complex perturbations can still create challenges with convergence, possibly requiring substantially longer simulation times and replicas. We therefore decide to consider all ligand pairs that occupy non-adjacent categories but which have a Tanimoto similarity of at least 0.7 when calculated using the Pairwise[43] fingerprint. This leaves us with 21 pairs of ligands for which to compute the FEP ΔΔG amongst our SSTR5 models.

Model generation proceeds similarly to what we described above for the SSTR2 and SSTR4 receptors. We generated five AlphaFold models of SSTR5 on March 3rd, 2022, preceding the release of any public SSTR experimental structures. For a template ligand, we align the ligand from PDB 6DDF, a μ-opioid structure, onto the AlphaFold models. For SSTR2 and SSTR4, we select the most potent ligand to dock in using IFD-MD but here, there are over 139 equally potent ligands all falling under the same category. Therefore, we chose to dock in 5 ligands using IFD-MD (ligands ***1-77, 1-78, 1-141, 1-192, 1-202***) in each of the 5 AlphaFold models.

Based on our expectation from comparisons with the SSTR2 and SSTR4 datasets reported above, a salt bridge will be necessary and indeed all ligands in this dataset offer a positive amine. Using the formation of a ligand-receptor salt-bridge as a filter, we arrive at 83 possible models, far larger than the 25 models we generate for SSTR2 and SSTR4 but evaluation here is cheaper since we are only computing single edge ΔΔGs for 21 ligand pairs. Applying our $RMSE_{lower\text{-}bound}$ metric, we rank the 83 models and select the top 10 models for running additional ligand pairs where the Tanimoto similarity cutoff is lowered from 0.7 to 0.65. This increases the number of ligand pairs from 21 to 54. The top model across these 54 ligand pairs has an $RMSE_{lower\text{-}bound}$ of 1.16 kcal/mol. Since we only compute ΔΔG's and lack a reference to convert to ΔG's, we cannot report an R^2; the $RMSE_{lower\text{-}bound}$ remains the only metric for model performance.

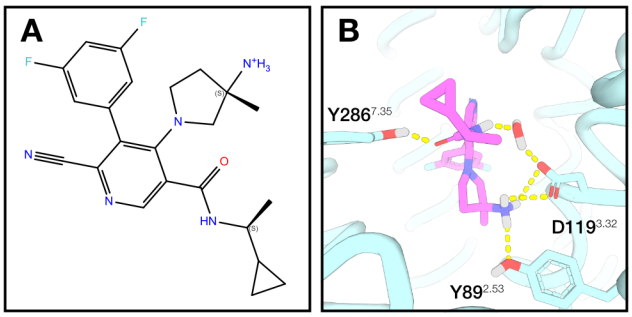

Figure 9. Final model of SSTR5 bound to ligand *1-77*. A) 2D representation of ligand *1-77*. B) The *1*-77 ligand bound in SSTR5. The model shows features similar to the SSTR4 model with a salt bridge and water mediated interactions from a ligand amide to D119.

Table 5. Results for the top 10 SSTR5 models ranked by $RMSE_{lower\_bound}$[a]

Model	Target Ligand	AlphaFold Model	IFD-MD Model	$RMSE_{lower\text{-}bound}$ (kcal/mol)	RMSD to Model 1 (Å)
1	1-77	1	1	1.16	0.00
2	1-192	2	2	1.30	1.99
3	1-202	3	1	1.32	1.34
4	1-78	3	3	1.35	1.76
5	1-141	1	3	1.36	1.24
6	1-141	1	4	1.37	1.76
7	1-77	1	5	1.38	1.33
8	1-78	4	1	1.39	1.07
9	1-77	1	2	1.44	1.07
10	1-141	1	1	1.55	1.00

a. $RMSE_{lower\text{-}bound}$ is computed over 54 ligand pairs. RMSD to model 1 is over all ligand-heavy atoms but excludes the cyclopropylethyl group whose position varies significantly between the models. The target ligand is the ligand which was explicitly docked in using IFD-MD into the respective AlphaFold model. Other ligands in the congeneric series are aligned to the IFD-MD output of docking that ligand.

Figure 9 shows the final SSTR5 model. It has features similar to our final SSTR4 model with a salt bridge and water mediated interaction to D119. We observe that the top 10 models all have very similar ligand binding modes with the most significant variation lying in the placement of the cyclopropylethyl group and the hydrophobic receptor residues it pairs with (Table 5). This reproducibly observed binding mode is seen when alternative ligands are docked into the AlphaFold models using IFD-MD and with alternative AlphaFold models. We consider this supportive of the hypothesis that this proposed binding mode is lying within a well-defined low-energy basin.

To date, no experimental structure of SSTR5 has been deposited in the PDB which leaves us without further opportunities for model validation. We look forward to future experimental

conformational or refutation of this model but presently this example serves as an opportunity to quantitatively explore the challenges of FEP-based model validated using a categorical dataset.

IV Discussion

The above modeling efforts provide an initial picture as to how an initial ensemble of candidate receptor structures (obtained from AlphaFold enumeration and/or experimental structure determination) can be combined with experimental binding affinity data for a congeneric series to produce a structural model that has been validated via FEP calculations suitable for advancing a structure-based drug discovery project. Note that different induced fit structures may well be required for different congeneric series. GPCRs have significant plasticity associated with both alternative side chain rotamer states, and small motions of one or more of the 7 transmembrane helices. Ideally, a project would have available multiple validated structures that could be used for both lead generation (via for example virtual screening) and lead optimization.

The results also reveal some limitations that can arise from the nature of the available experimental data. For SSTR2, the small number of ligands in the series preclude unambiguous identification of the correct binding mode; however, as pointed out above, this limitation could readily be overcome by synthesizing and testing additional compounds, designed to differentiate between the two models. We have used such strategies effectively in previous internal projects when investigating other types of receptors.

The SSTR5 study investigates the effect of a different type of limitation, namely the availability of only categorical ligand classification rather than accurate binding affinity measurements. For the case studied here, the data was (apparently) sufficient to overcome the ambiguities associated with this sort of experimental noise. The similarity in binding mode of the top 10 structures, suggests that perhaps there were fewer reasonable alternatives available than in for example the SSTR2 case study.

A final observation emphasizes that it is essential to rigorously assess the correct protonation and tautomer states for the ligand series if reliable conclusions are to be drawn from an IFD-MD/FEP approach. For the SSTR4 dataset, the pKa of the oxazepine nitrogen is not straightforward to compute reliably via the Jaguar Macro pKa algorithm. As part of the pKa prediction, the lowest energy conformer in solution (implicit solvent) and gas phase must be found. Hence the predictions are a function of the number of conformers evaluated in Jaguar and potential artifacts, such as over predicting the formation of an internal charged hydrogen bonds in implicit solvent[44]. Truncating the ligand far from the oxazepine can improve the accuracy of the prediction by focusing sampling on groups that can influence the pKa. In Table 6 below, we show results obtained from various pKa calculation approaches for a single ligand. We ultimately select the most aggressive truncation (isoquinoline gem-dimethyl truncated to methyl for the ligand in Figure 2B). This truncated form, used with the nitrogen walk on the fused phenyl ring, is generalizable across the SSTR4 ligand series.

Table 6. Comparison of pKa predictions as a function of the amount of conformational sampling or degree of truncation of the molecule.

Macro-pKa Input	Predicted pKa
Complete Ligand (5 conformers)	4.42
Complete Ligand (20 conformers)	5.60
Complete Ligand (50 conformers)	5.63
Truncated (Isoquinoline gem-dimethyl to t-butyl)	5.94
Truncated (Isoquinoline gem-dimethyl to methyl)	6.17
Complete Ligand (isoquinoline mutated to naphthalene)	5.78

While we believe that the Jaguar Macro pKa results are sufficiently accurate, experimental validation of this assertion would be important if one were working on an actual structure-based project. The effects of simply ignoring the pKa correction (or, equivalently, concluding that the nitrogen is protonated in solution for all members of the series), is shown in the table of FEP results in Table S5. A completely different binding mode, (AF2, IFD1) shown in Figure S3, would be selected in this case, rather than the top model after pKa correction (AF5, IFD1) (Figure 4). This binding mode has an RMSD of 6.5 Å to our final model.

V Conclusion

We have demonstrated that the IFD-MD methodology of ref. [6] performs accurately and robustly for retrospective GPCR induced fit ligand docking, and then applied this approach, in conjunction with FEP, to three GPCR drug targets of interest for which experimental structures binding the ligand series studied here do not currently exist. Our results constitute prospective prediction of the binding modes of the series in each case, which await validation (or refutation) via experimental structure determination.

While enormous strides have been made in utilizing FEP to drive structure-based drug design projects[26,45], the domain of applicability has previously been limited to receptors for which high resolution crystal or cryo-EM structures can be readily obtained. Note that a single structural starting point is often not adequate; a typical application involves obtaining multiple experimental structures to check whether there has been any change in the binding mode as lead optimization proceeds.

When structure determination is difficult or impossible, the traditional approach to drug discovery has been a ligand-based methodology, in which QSAR modeling of ligand series (nowadays using modern machine learning methods) provides guidance for population of the synthesis queue. With the advent of rapidly improving experimental structure determination methods, and the availability of AlphaFold structures for, in principle, every protein target in the human genome, the question is raised as to whether some sort of structure-based approach should be followed for all targets, on the theory that the structural information available can be profitably used, even if it is limited in quantity and incomplete.

The approach we describe above represents a synthesis of ligand-based and structure-based information (with the former being incorporated into the model via the IFD-MD and FEP+ cal-

culations) which we believe has great promise in upgrading discovery efforts for targets that formerly have been pursued using a purely ligand-based approach. While the robustness of binding affinity predictions may not be quite as good as in the ideal situation of readily available high resolution experimental structures of arbitrary protein-ligand complexes, the relevant question is whether it represents an improvement on a purely ligand-based prediction. The results shown above certainly suggest that this is indeed the case.

ASSOCIATED CONTENT

Supporting Information

Detailed results for the retrospective GPCR crossdocks using IFD-MD or GlideSP, pKa values and the associated ΔG corrections at pH 7.4 used for the SSTR4 ligand dataset, FEP results on AlphaFold or experimentally derived SSTR2 models, SSTR4 FEP results when no pKa correction is applied, comparison of the best performing SSTR4 models with and without applying pKa corrections, SSTR4 modeling using rigid-receptor docking (PDF)

Coordinates of the final SSTR4 model (PDB)
Coordinates of the final SSTR5 model (PDB)
Coordinates of the final SSTR2 model (PDB)

AUTHOR INFORMATION

Corresponding Author

* Edward B. Miller – Email: Ed.Miller@schrodinger.com

Author Contributions

The manuscript was written through contributions of all authors. / All authors have given approval to the final version of the manuscript.

Notes

The authors declare the following competing financial interest(s): R.A.F. has a significant financial stake in Schrödinger, Inc., is a consultant to Schrödinger, Inc., and is on the Scientific Advisory Board of Schrödinger, Inc.

ABBREVIATIONS

SSTR4, Somatostatin Receptor Type 4; IFD-MD, Induced-Fit Docking Molecular Dynamics; AF5, IFD1, The top ranked IFD-MD where docking is performed using the 5th ranked AlphaFold prediction;

REFERENCES

(1) Sriram, K.; Insel, P. A. G Protein-Coupled Receptors as Targets for Approved Drugs: How Many Targets and How Many Drugs? *Mol. Pharmacol.* **2018**, *93* (4), 251–258. https://doi.org/10.1124/mol.117.111062.

(2) Isberg, V.; Vroling, B.; van der Kant, R.; Li, K.; Vriend, G.; Gloriam, D. GPCRDB: An Information System for G Protein-Coupled Receptors. *Nucleic Acids Res.* **2014**, *42* (D1), D422–D425. https://doi.org/10.1093/nar/gkt1255.

(3) Jumper, J.; Evans, R.; Pritzel, A.; Green, T.; Figurnov, M.; Ronneberger, O.; Tunyasuvunakool, K.; Bates, R.; Žídek, A.; Potapenko, A.; Bridgland, A.; Meyer, C.; Kohl, S. A. A.; Ballard, A. J.; Cowie, A.; Romera-Paredes, B.; Nikolov, S.; Jain, R.; Adler, J.; Back, T.; Petersen, S.; Reiman, D.; Clancy, E.; Zielinski, M.; Steinegger, M.; Pacholska, M.; Berghammer, T.; Bodenstein, S.; Silver, D.; Vinyals, O.; Senior, A. W.; Kavukcuoglu, K.; Kohli, P.; Hassabis, D. Highly Accurate Protein Structure Prediction with AlphaFold. *Nature* **2021**, *596* (7873), 583–589. https://doi.org/10.1038/s41586-021-03819-2.

(4) Beuming, T.; Martín, H.; Díaz-Rovira, A. M.; Díaz, L.; Guallar, V.; Ray, S. S. Are Deep Learning Structural Models Sufficiently Accurate for Free-Energy Calculations? Application of FEP+ to AlphaFold2-Predicted Structures. *J. Chem. Inf. Model.* **2022**, *62* (18), 4351–4360. https://doi.org/10.1021/acs.jcim.2c00796.

(5) Lenselink, E. B.; Louvel, J.; Forti, A. F.; van Veldhoven, J. P. D.; de Vries, H.; Mulder-Krieger, T.; McRobb, F. M.; Negri, A.; Goose, J.; Abel, R.; van Vlijmen, H. W. T.; Wang, L.; Harder, E.; Sherman, W.; IJzerman, A. P.; Beuming, T. Predicting Binding Affinities for GPCR Ligands Using Free-Energy Perturbation. *ACS Omega* **2016**, *1* (2), 293–304. https://doi.org/10.1021/acsomega.6b00086.

(6) Miller, E. B.; Murphy, R. B.; Sindhikara, D.; Borrelli, K. W.; Grisewood, M. J.; Ranalli, F.; Dixon, S. L.; Jerome, S.; Boyles, N. A.; Day, T.; Ghanakota, P.; Mondal, S.; Rafi, S. B.; Troast, D. M.; Abel, R.; Friesner, R. A. Reliable and Accurate Solution to the Induced Fit Docking Problem for Protein–Ligand Binding. *J. Chem. Theory Comput.* **2021**, *17* (4), 2630–2639. https://doi.org/10.1021/acs.jctc.1c00136.

(7) Juliana, C. A.; Chai, J.; Arroyo, P.; Rico-Bautista, E.; Betz, S. F.; De León, D. D. A Selective Nonpeptide Somatostatin Receptor 5 Agonist Effectively Decreases Insulin Secretion in Hyperinsulinism. *J. Biol. Chem.* **2023**, *299* (6), 104816. https://doi.org/10.1016/j.jbc.2023.104816.

(8) Zhao, J.; Wang, S.; Markison, S.; Kim, S. H.; Han, S.; Chen, M.; Kusnetzow, A. K.; Rico-Bautista, E.; Johns, M.; Luo, R.; Struthers, R. S.; Madan, A.; Zhu, Y.; Betz, S. F. Discovery of Paltusotine (CRN00808), a Potent, Selective, and Orally Bioavailable Non-Peptide SST2 Agonist. *ACS Med. Chem. Lett.* **2023**, *14* (1), 66–74. https://doi.org/10.1021/acsmedchemlett.2c00431.

(9) Bo, Q.; Yang, F.; Li, Y.; Meng, X.; Zhang, H.; Zhou, Y.; Ling, S.; Sun, D.; Lv, P.; Liu, L.; Shi, P.; Tian, C. Structural Insights into the Activation of Somatostatin Receptor 2 by Cyclic SST Analogues. *Cell Discov.* **2022**, *8* (1), 47. https://doi.org/10.1038/s41421-022-00405-2.

(10) Zhao, J.; Fu, H.; Yu, J.; Hong, W.; Tian, X.; Qi, J.; Sun, S.; Zhao, C.; Wu, C.; Xu, Z.; Cheng, L.; Chai, R.; Yan, W.; Wei, X.; Shao, Z. Prospect of Acromegaly Therapy: Molecular Mechanism of Clinical Drugs Octreotide and Paltusotine. *Nat. Commun.* **2023**, *14* (1), 962. https://doi.org/10.1038/s41467-023-36673-z.

(11) Chen, S.; Teng, X.; Zheng, S. Molecular Basis for the Selective G Protein Signaling of Somatostatin Receptors. *Nat. Chem. Biol.* **2023**, *19* (2), 133–140. https://doi.org/10.1038/s41589-022-01130-3.

(12) Zhao, W.; Han, S.; Qiu, N.; Feng, W.; Lu, M.; Zhang, W.; Wang, M.; Zhou, Q.; Chen, S.; Xu, W.; Du, J.; Chu, X.; Yi, C.; Dai, A.; Hu, L.; Shen, M. Y.; Sun, Y.; Zhang, Q.; Ma, Y.; Zhong, W.; Yang, D.; Wang, M.-W.; Wu, B.; Zhao, Q. Structural Insights into Ligand Recognition and Selectivity of Somatostatin Receptors. *Cell Res.* **2022**, *32* (8), 761–772. https://doi.org/10.1038/s41422-022-00679-x.

(13) Shindyalov, I. N.; Bourne, P. E. Protein Structure Alignment by Incremental Combinatorial Extension (CE) of the Optimal Path. *Protein Eng.* **1998**, *11* (9), 739–747.

(14) Schrödinger Release 2023-1: Protein Preparation Wizard, 2023.

(15) Xu, T.; Zhu, K.; Beautrait, A.; Vendome, J.; Borrelli, K. W.; Abel, R.; Friesner, R. A.; Miller, E. B. Induced-Fit Docking Enables Accurate Free Energy Perturbation Calculations in Homology Models. *J. Chem. Theory Comput.* **2022**, *18* (9), 5710–5724. https://doi.org/10.1021/acs.jctc.2c00371.

(16) Murphy, R. B.; Repasky, M. P.; Greenwood, J. R.; Tubert-Brohman, I.; Jerome, S.; Annabhimoju, R.; Boyles, N. A.; Schmitz, C. D.; Abel, R.; Farid, R.; Friesner, R. A. WScore: A Flexible and Accurate Treatment of Explicit Water Molecules in Ligand–Receptor Docking. *J. Med. Chem.* **2016**, *59* (9), 4364–4384. https://doi.org/10.1021/acs.jmedchem.6b00131.

(17) Clark, A. J.; Tiwary, P.; Borrelli, K.; Feng, S.; Miller, E. B.; Abel, R.; Friesner, R. A.; Berne, B. J. Prediction of Protein–Ligand Binding Poses via a Combination of Induced Fit Docking and Metadynamics Simulations. *J. Chem. Theory Comput.* **2016**, *12* (6), 2990–2998. https://doi.org/10.1021/acs.jctc.6b00201.

(18) Lomize, M. A.; Lomize, A. L.; Pogozheva, I. D.; Mosberg, H. I. OPM: Orientations of Proteins in Membranes Database. *Bioinformatics* **2006**, *22* (5), 623–625. https://doi.org/10.1093/bioinformatics/btk023.
(19) Li, J.; Abel, R.; Zhu, K.; Cao, Y.; Zhao, S.; Friesner, R. A. The VSGB 2.0 Model: A next Generation Energy Model for High Resolution Protein Structure Modeling. *Proteins Struct. Funct. Bioinforma.* **2011**, *79* (10), 2794–2812. https://doi.org/10.1002/prot.23106.
(20) Schrödinger Release 2020-3: Desmond Molecular Dynamics System, 2020.
(21) Bowers, K. J.; Chow, E.; Xu, H.; Dror, R. O.; Eastwood, M. P.; Gregerson, B. A.; Klepeis, J. L.; Kolossvary, I.; Moraes, M. A.; Sacerdoti, F. D.; Salmon, J. K.; Shan, Y.; Shaw, D. E. Proceedings of the 2006 ACM/IEEE Conference on Supercomputing, SC'06. In *Proceedings of the 2006 ACM/IEEE Conference on Supercomputing, SC'06*; Association for Computing Machinery: New York, NY, USA, 2006.
(22) Schrödinger Release 2023-1: Desmond Molecular Dynamics System, 2023.
(23) Ross, G. A.; Russell, E.; Deng, Y.; Lu, C.; Harder, E. D.; Abel, R.; Wang, L. Enhancing Water Sampling in Free Energy Calculations with Grand Canonical Monte Carlo. *J. Chem. Theory Comput.* **2020**, *16* (10), 6061–6076. https://doi.org/10.1021/acs.jctc.0c00660.
(24) Tikhonova, I. G.; Gigoux, V.; Fourmy, D. Understanding Peptide Binding in Class A G Protein-Coupled Receptors. *Mol. Pharmacol.* **2019**, *96* (5), 550–561. https://doi.org/10.1124/mol.119.115915.
(25) Mazzaferro, R.; Ferrara, M.; Giovannini, R. Aryl and Heteroaryl-Fused Tetrahydro-1,4-Oxazepine Amides as Somatostatin Receptor Subtype 4 (SSTR4) Agonists. US10183940B2, 2015.
(26) Wang, L.; Wu, Y.; Deng, Y.; Kim, B.; Pierce, L.; Krilov, G.; Lupyan, D.; Robinson, S.; Dahlgren, M. K.; Greenwood, J.; Romero, D. L.; Masse, C.; Knight, J. L.; Steinbrecher, T.; Beuming, T.; Damm, W.; Harder, E.; Sherman, W.; Brewer, M.; Wester, R.; Murcko, M.; Frye, L.; Farid, R.; Lin, T.; Mobley, D. L.; Jorgensen, W. L.; Berne, B. J.; Friesner, R. A.; Abel, R. Accurate and Reliable Prediction of Relative Ligand Binding Potency in Prospective Drug Discovery by Way of a Modern Free-Energy Calculation Protocol and Force Field. *J. Am. Chem. Soc.* **2015**, *137* (7), 2695–2703. https://doi.org/10.1021/ja512751q.
(27) Contour-Galcéra, M.-O.; Sidhu, A.; Plas, P.; Roubert, P. 3-Thio-1,2,4-Triazoles, Novel Somatostatin Sst2/Sst5 Agonists. *Bioorg. Med. Chem. Lett.* **2005**, *15* (15), 3555–3559. https://doi.org/10.1016/j.bmcl.2005.05.061.
(28) Clark, A. J.; Gindin, T.; Zhang, B.; Wang, L.; Abel, R.; Murret, C. S.; Xu, F.; Bao, A.; Lu, N. J.; Zhou, T.; Kwong, P. D.; Shapiro, L.; Honig, B.; Friesner, R. A. Free Energy Perturbation Calculation of Relative Binding Free Energy between Broadly Neutralizing Antibodies and the Gp120 Glycoprotein of HIV-1. *J. Mol. Biol.* **2017**, *429* (7), 930–947. https://doi.org/10.1016/j.jmb.2016.11.021.
(29) Cappel, D.; Hall, M. L.; Lenselink, E. B.; Beuming, T.; Qi, J.; Bradner, J.; Sherman, W. Relative Binding Free Energy Calculations Applied to Protein Homology Models. *J. Chem. Inf. Model.* **2016**, *56* (12), 2388–2400. https://doi.org/10.1021/acs.jcim.6b00362.
(30) Moraca, F.; Negri, A.; de Oliveira, C.; Abel, R. Application of Free Energy Perturbation (FEP+) to Understanding Ligand Selectivity: A Case Study to Assess Selectivity Between Pairs of Phosphodiesterases (PDE's). *J. Chem. Inf. Model.* **2019**, *59* (6), 2729–2740. https://doi.org/10.1021/acs.jcim.9b00106.
(31) Clark, A. J.; Negron, C.; Hauser, K.; Sun, M.; Wang, L.; Abel, R.; Friesner, R. A. Relative Binding Affinity Prediction of Charge-Changing Sequence Mutations with FEP in Protein–Protein Interfaces. *J. Mol. Biol.* **2019**, *431* (7), 1481–1493. https://doi.org/10.1016/j.jmb.2019.02.003.
(32) Schrödinger Release 2021-4: FEP+. Schrodinger, Inc: New York, NY 2020.
(33) Liu, S.; Wu, Y.; Lin, T.; Abel, R.; Redmann, J. P.; Summa, C. M.; Jaber, V. R.; Lim, N. M.; Mobley, D. L. Lead Optimization Mapper: Automating Free Energy Calculations for Lead Optimization. *J. Comput. Aided Mol. Des.* **2013**, *27* (9), 755–770. https://doi.org/10.1007/s10822-013-9678-y.
(34) Vale, W.; Rivier, J.; Ling, N.; Brown, M. Biologic and Immunologic Activities and Applications of Somatostatin Analogs. *Somatostat. Symp.* **1978**, *27* (9, Supplement 1), 1391–1401. https://doi.org/10.1016/0026-0495(78)90081-1.
(35) Zhao, W.; Han, S.; Qiu, N.; Feng, W.; Lu, M.; Zhang, W.; Wang, M.; Zhou, Q.; Chen, S.; Xu, W.; Du, J.; Chu, X.; Yi, C.; Dai, A.; Hu, L.; Shen, M. Y.; Sun, Y.; Zhang, Q.; Ma, Y.; Zhong, W.; Yang, D.; Wang, M.-W.; Wu, B.; Zhao, Q. Structural Insights into Ligand Recognition and Selectivity of Somatostatin Receptors. *Cell Res.* **2022**, *32* (8), 761–772. https://doi.org/10.1038/s41422-022-00679-x.
(36) Mazzaferro, R.; Ferrara, M.; Giovannini, R. Aryl and Heteroaryl-Fused Tetrahydro-1,4-Oxazepine Amides as Somatostatin Receptor Subtype 4 (SSTR4) Agonists, 2015.
(37) Zhao, Jian, Z., Yunfci, Wang, Shimiao, Chen Mi, Pontillo, Joseph. Nonpeptide Somatostatin Type 5 Receptor Agonists and Uses Thereof.
(38) Tang, H.; Jensen, K.; Houang, E.; McRobb, F. M.; Bhat, S.; Svensson, M.; Bochevarov, A.; Day, T.; Dahlgren, M. K.; Bell, J. A.; Frye, L.; Skene, R. J.; Lewis, J. H.; Osborne, J. D.; Tierney, J. P.; Gordon, J. A.; Palomero, M. A.; Gallati, C.; Chapman, R. S. L.; Jones, D. R.; Hirst, K. L.; Sephton, M.; Chauhan, A.; Sharpe, A.; Tardia, P.; Dechaux, E. A.; Taylor, A.; Waddell, R. D.; Valentine, A.; Janssens, H. B.; Aziz, O.; Bloomfield, D. E.; Ladha, S.; Fraser, I. J.; Ellard, J. M. Discovery of a Novel Class of D-Amino Acid Oxidase Inhibitors Using the Schrödinger Computational Platform. *J. Med. Chem.* **2022**, *65* (9), 6775–6802. https://doi.org/10.1021/acs.jmedchem.2c00118.
(39) Schrödinger Release 2023-2: Jaguar, 2023.
(40) de Oliveira, C.; Yu, H. S.; Chen, W.; Abel, R.; Wang, L. Rigorous Free Energy Perturbation Approach to Estimating Relative Binding Affinities between Ligands with Multiple Protonation and Tautomeric States. *J. Chem. Theory Comput.* **2019**, *15* (1), 424–435. https://doi.org/10.1021/acs.jctc.8b00826.
(41) Chen, W.; Cui, D.; Jerome, S. V.; Michino, M.; Lenselink, E. B.; Huggins, D. J.; Beautrait, A.; Vendome, J.; Abel, R.; Friesner, R. A.; Wang, L. Enhancing Hit Discovery in Virtual Screening through Absolute Protein–Ligand Binding Free-Energy Calculations. *J. Chem. Inf. Model.* **2023**, *63* (10), 3171–3185. https://doi.org/10.1021/acs.jcim.3c00013.
(42) Friesner, R. A.; Banks, J. L.; Murphy, R. B.; Halgren, T. A.; Klicic, J. J.; Mainz, D. T.; Repasky, M. P.; Knoll, E. H.; Shelley, M.; Perry, J. K.; Shaw, D. E.; Francis, P.; Shenkin, P. S. Glide: A New Approach for Rapid, Accurate Docking and Scoring. 1. Method and Assessment of Docking Accuracy. *J. Med. Chem.* **2004**, *47* (7), 1739–1749. https://doi.org/10.1021/jm0306430.
(43) Carhart, R. E.; Smith, D. H.; Venkataraghavan, R. Atom Pairs as Molecular Features in Structure-Activity Studies: Definition and Applications. *J Chem Inf Comput Sci* **1985**, *25*, 64–73.
(44) Yu, Z.; Jacobson, M. P.; Josovitz, J.; Rapp, C. S.; Friesner, R. A. First-Shell Solvation of Ion Pairs: Correction of Systematic Errors in Implicit Solvent Models. *J. Phys. Chem. B* **2004**, *108* (21), 6643–6654. https://doi.org/10.1021/jp037821l.
(45) Schindler, C. E. M.; Baumann, H.; Blum, A.; Böse, D.; Buchstaller, H.-P.; Burgdorf, L.; Cappel, D.; Chekler, E.; Czodrowski, P.; Dorsch, D.; Eguida, M. K. I.; Follows, B.; Fuchß, T.; Grädler, U.; Gunera, J.; Johnson, T.; Jorand Lebrun, C.; Karra, S.; Klein, M.; Knehans, T.; Koetzner, L.; Krier, M.; Leiendecker, M.; Leuthner, B.; Li, L.; Mochalkin, I.; Musil, D.; Neagu, C.; Rippmann, F.; Schiemann, K.; Schulz, R.; Steinbrecher, T.; Tanzer, E.-M.; Unzue Lopez, A.; Viacava Follis, A.; Wegener, A.; Kuhn, D. Large-Scale Assessment of Binding Free Energy Calculations in Active Drug Discovery Projects. *J. Chem. Inf. Model.* **2020**, *60* (11), 5457–5474. https://doi.org/10.1021/acs.jcim.0c00900.